ISSN: 0975-833X

Available online at http://www.journalcra.com

International Journal of Current Research
Vol. 18, Issue, 06, pp.37469-37475, June, 2026
DOI: https://doi.org/10.24941/ijcr.50646.06.2026

INTERNATIONAL JOURNAL OF CURRENT RESEARCH

RESEARCH ARTICLE

EXPERIMENTAL AND THEORETICAL STUDY OF THE CORROSION INHIBITION OF ALUMINUM IN SULFURIC ACID MEDIA BY 2-(2-(4-CHLOROBENZYLIDENE) HYDRAZINYL)-3-NITROIMIDAZO (1,2-A) PYRIDINE

KOUAME Tanoh Stanley[1], EHOUMAN Ahissan Donatien[2]*, AKPATAKU Kossitse Venyo[3], FATOGOMA Diarrassouba[4] and Niamien Paulin Marius[1]

[1]Laboratoire de Réaction et Constitution de la Matière, Université Félix Houphouët BOIGNY 22 BP 582 Abidjan 22, Côte d'Ivoire; [2]Laboratoire de Thermodynamique et Physico-Chimie du Milieu, Université NANGUI ABROGOUA, 02 BP 801 Abidjan 02, Côte d'Ivoire; [3]Laboratoire de Chimie Organique et Sciences de l'Environnementales (LaCOSE), Faculté des Sciences et Techniques, Université de Kara, BP 404, Kara, Togo; [4]Unité de Formation et de Recherche Sciences et Technologie (UFR-ST),Université Alassane OUATTARA, 01 BP 18 Bouaké 01, Côte d'Ivoire

ARTICLE INFO

Article History:
Received 27th March, 2026
Received in revised form
24th April, 2026
Accepted 25th May, 2026
Published online 30th June, 2026

Keywords:
Aluminum, 2-(2-(4-chlorobenzylidene)hydrazinyl)-3-nitroimidazo(1,2-α)pyridine, corrosion inhibition, Density Functional Theory (DFT), gravimetry.

Corresponding author:
EHOUMAN Ahissan Donatien

ABSTRACT

The objective of this study is to test the corrosion inhibition efficacy of the molecule 2-(2-(4-chlorobenzylidene)hydrazinyl)-3-nitroimidazo(1,2-α)pyridine, or 4Cl-BNH-NIP, on aluminum corrosion in a sulfuric acid medium using the mass loss method. The corrosion inhibition efficiency (EI) increases with increasing concentration but decreases with rising temperature of the corrosive medium. In a sulfuric acid medium, 4Cl-BNH-NIP exhibits 100 % inhibition efficiency at 298 K and 308 K starting at 0.001 mmol/L, and 78.92 % at 338 K at 0.5 mmol/L. DFT calculations using the 6-311G (d,p) basis set revealed the attack sites of the molecules. Predictive formulas were established based on their principal quantum components.

Citation: KOUAME Tanoh Stanley, EHOUMAN Ahissan Donatien, AKPATAKU Kossitse Venyo, FATOGOMA Diarrassouba4 and Niamien Paulin Marius. 2026. "Experimental and Theoretical Study of the Corrosion Inhibition of Aluminum in Sulfuric Acid Media by 2-(2-(4-chlorobenzylidene) hydrazinyl)-3-nitroimidazo(1,2-α)pyridine...". ***International Journal of Current Research, 18, (06), 37469-37475.***

INTRODUCTION

Aluminum (1,2), widely used in infrastructure, transportation, and various industries due to its remarkable properties, remains susceptible to corrosion in acidic and chlorinated environments (3,4). This phenomenon has significant economic, environmental, and safety implications, with an estimated cost of 3.4% of global GDP (5,6). To mitigate these effects, the use of corrosion inhibitors is an effective solution. Among these, organic compounds from the benzimidazole family are of particular interest due to their inhibitory efficacy and their potential environmental friendliness (7). Several studies have demonstrated their ability to adsorb onto metal surfaces and reduce the corrosion rate (7,8). Inhibitory performance is generally evaluated using gravimetric and electrochemical methods (9). With a view to environmental protection, reducing experimental costs, and ensuring safety, the QSPR method has been considered. It allows the properties of a molecule to be linked to its structure in order to predict the behavior of similar compounds (10). This approach is based on establishing mathematical relationships between the properties to be predicted and the quantum, physicochemical, and thermodynamic descriptors of the molecules under study.

MATERIALS AND METHODS

Aluminum Specimens : The samples studied were commercial aluminum rods (98 % purity) measuring 10 mm in length and 2 mm in diameter. The inhibitor used, 4Cl-BNH-NIP (2-(2-(4-chlorobenzylidene)hydrazineyl) -3-nitroimidazo(1,2-α)pyridine), is a molecule synthesized by aldolization of 2-hydrazineyl-3-nitroimidazo(1,2-α)pyridine with 4-chlorobenzaldehyde (99.99 %). Its molecular formula is $C_{14}H_{10}ClN_5O_2$ and its molar mass is 315.72 g/mol.

Synthesis of the Target Molecule

Reagents for Organic Synthesis: To synthesize the organic compound in this study, we required the following reagents: Phosphorus (V) oxychloride, 2-aminopyridine, benzaldehyde, parachlorobenzaldehyde, 2-hydroxybenzaldehyde, hydrazine, triethylamine, ethanol, toluene, nitric acid, and sulfuric acid.

Synthesis steps. The synthesis was carried out in five steps according to the protocol proposed by Adingra et al (11).

Step 1: This step involved reacting 2-aminopyridine with chloroacetic acid in the presence of ethanol and triethylamine under reflux for 5 hours.

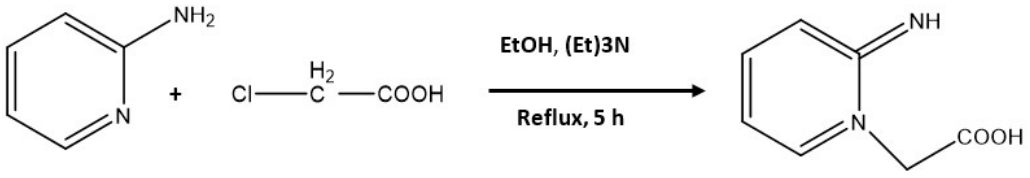

2-(2-imino-1λ⁴,2λ⁵-pyridin-1-yl)acetic acid

80 %

The precipitated product was filtered and then washed with ethanol. After drying, we obtained a white solid with a yield of 80%.

Step 2: In this step, we reacted the product obtained in the first step with phosphorus(V) oxychloride in the presence of toluene under reflux for 16 hours. At the end of the reaction, the reaction mixture was cooled to room temperature. The reaction mixture was then neutralized with a 10% sodium hydroxide solution. After treating the reaction mixture, the organic phase was extracted with ethyl acetate and then evaporated under reduced pressure. The resulting residue is then purified by silica gel chromatography using hexane/ethyl acetate (60/40) as the eluent. After drying, we obtained 2-chloroimidazo(1,2-α)pyridine as a white solid with a yield of 82%.

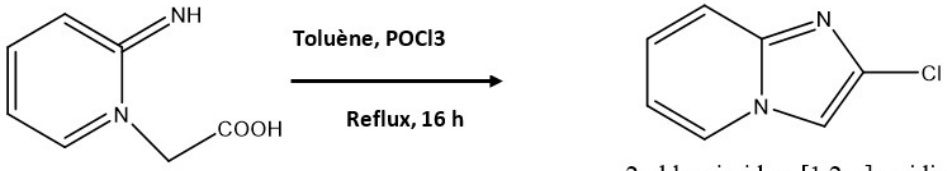

2-chloroimidazo[1,2-*a*]pyridine

Step 3: In this step, we reacted the product formed in step 2 with nitric acid in the presence of sulfuric acid according to the following equation:

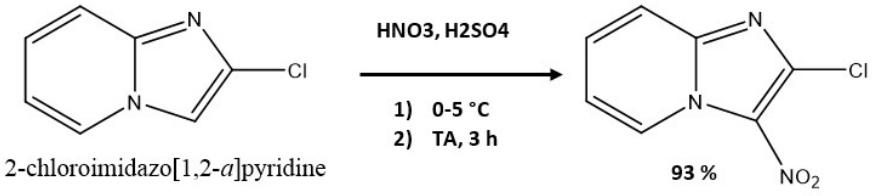

2-chloroimidazo[1,2-*a*]pyridine

2-chloro-3-nitroimidazo[1,2-*a*]pyridine

After treatment of the reaction mixture and purification, 2-chloro-3-nitroimidazo(1,2-α)pyridine was isolated as a yellowish solid with a yield of 93 %.

Step 4: This step led to the formation of our starting molecule in this organic synthesis process. We reacted the product obtained in Step 3 (2-chloro-3-nitroimidazo(1,2-α)pyridine) with hydrazine in the presence of ethanol and water at 60–70 °C for 20 minutes to obtain 2-hydrazinyl-3 -nitroimidazo(1,2-α)pyridine, with which we reacted benzaldehyde derivatives to form our potential organic inhibitors. The product, after treatment and purification, was obtained with a 78% yield.

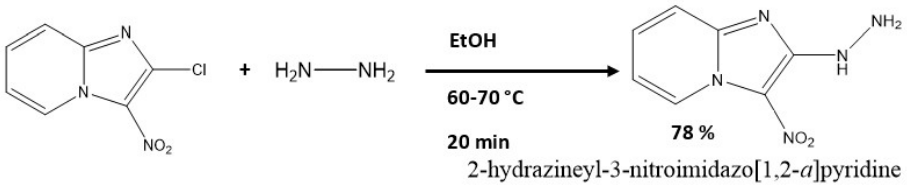

2-hydrazineyl-3-nitroimidazo[1,2-*a*]pyridine

The final step is the aldolization of our starting molecule, 2-hydrazinyl-3-nitroimidazo(1,2-α)pyridine.

Step 5: This step involved reacting benzaldehydes with our base under reflux for 30 minutes in methanol in the presence of two drops of acetic acid. After 30 minutes, the precipitate formed is filtered through a funnel and washed with methanol. The resulting molecules all have a yellowish appearance.

Synthesis of 2-(2-(4-chlorobenzylidene)hydrazinyl)-3-nitroimidazo(1,2-α)pyridine (CNIPY)

To obtain this molecule, we performed the aldolization of 2-hydrazineyl-3-nitroimidazo(1,2-α)pyridine with 4-chlorobenzaldehyde according to the equation

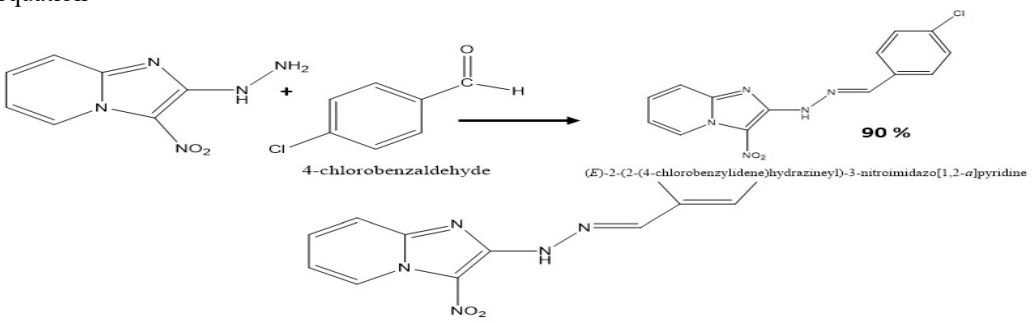

Figure 1. Molecular structure of 4Cl-BNH-NIP

Prepared Solutions : A hydrochloric acid solution was prepared by diluting a commercial 1 M hydrochloric acid solution with distilled water. The data for sulfuric acid are: d = 1.84 g/mL and P = 97%. The prepared 4Cl-BNH-NIP solutions have concentrations of C = 0.001 mM, C = 0.005 mM, C = 0.01 mM, C = 0.05 mM, C = 0.1 mM, and C = 0.5 mM.

Gravimetric Method : The gravimetric method (12–14), widely used to study corrosion inhibition due to its simplicity and reliability, involves immersing a pre-weighed metal sample in a test solution at temperatures between 298 K and 338 K. After a specified exposure time, the sample is rinsed, dried, and then reweighed. The resulting mass loss is used to determine the corrosion rate, the inhibitory efficiency, and the coverage rate using the appropriate equations.

$$W = \frac{\Delta m}{St} \quad (1)$$

$$EI(\%) = \frac{W_0 - W}{W_0} \times 100 \quad (2)$$

$$\theta = \frac{W_0 - W}{W_0} \quad (3)$$

Where W_0 and W are the corrosion rates in the absence and presence of the inhibitor, respectively; Δm is the mass loss, S is the total surface area of the copper sample, and t is the immersion time.

Quantum calculation method : Density functional theory (DFT) calculations were performed using various steps, including a graphical representation of the geometry of each molecule using the Gaussview visualization interface, and the application of a theoretical method (DFT) implemented in the commercial software Gaussian (15–17).

RESULTS AND DISCUSSION

Effects of Concentration and Temperature in H_2SO_4

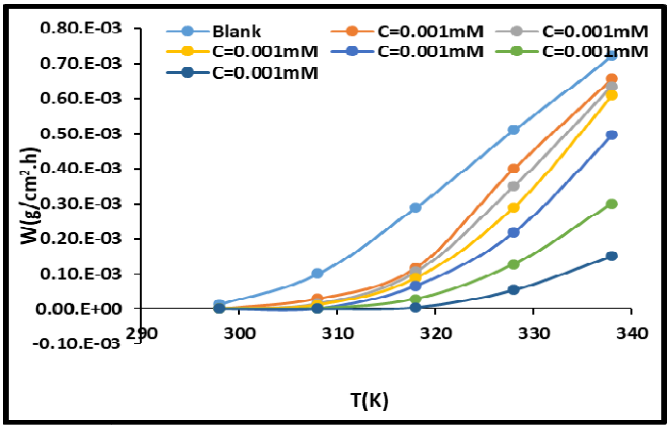

Figures 2 and 3 show, respectively, the evolution of the corrosion inhibition rate as a function of temperature and 4Cl-BNH-NIP concentration

Figure 2: Curve showing the corrosion rate as a function of temperature for different concentrations of the 4Cl-BNH-NIP molecule in an H_2SO_4 solution. Looking at the curve above, we observe that the corrosion rate, for a given inhibitor concentration, increases as the temperature rises, but that this increase in corrosion rate is relatively small (18).

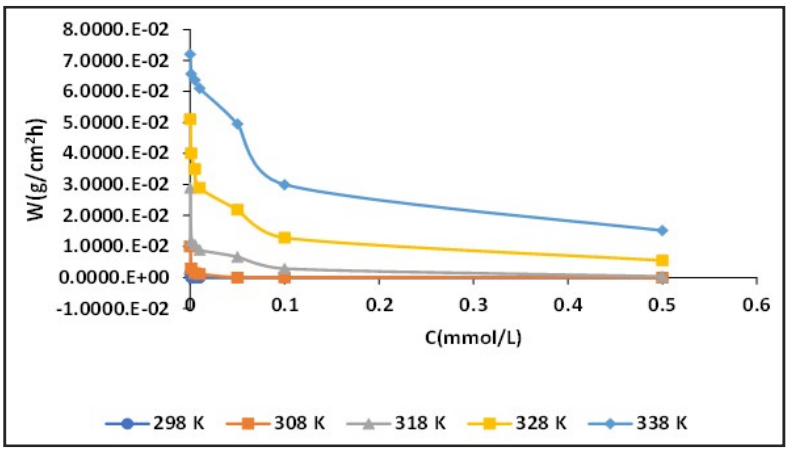

Figure 3: Curve showing the corrosion rate as a function of concentration for 4Cl-BNH-NIP at various temperatures in H_2SO_4.

We observe that the corrosion rate generally decreases as the inhibitor concentration increases at a fixed temperature in a sulfuric acid medium; these results are consistent with those obtained by Hadja et al. in similar studies conducted in a nitric acid medium (19).

Effects of Inhibitory Efficiency on Concentration and Temperature in H_2SO_4 : Figures 4 and 5 show, respectively, the variation in inhibitory efficiency as a function of temperature and 4Cl-BNH-NIP concentration.

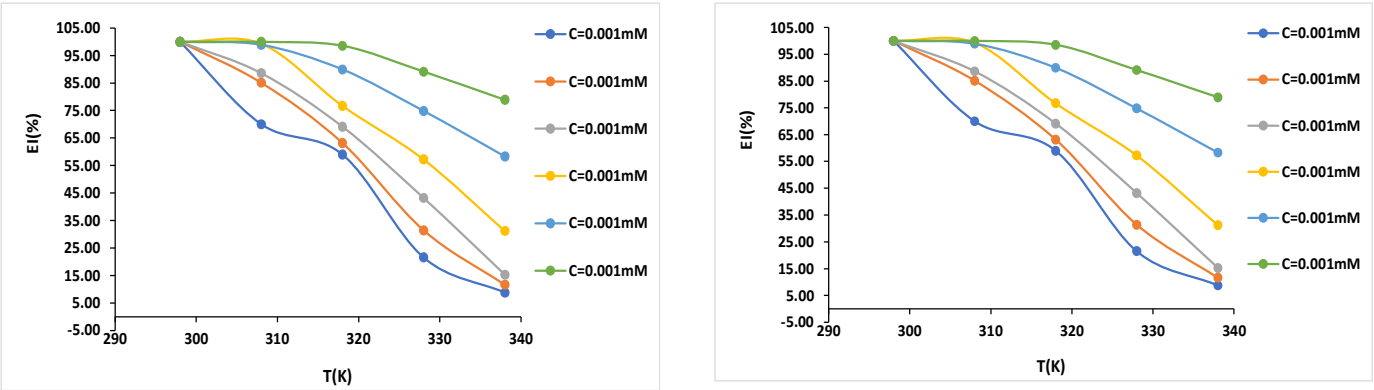

Figure 4. Inhibition efficiency as a function of temperature for different concentrations of 4Cl-BNH-NIP

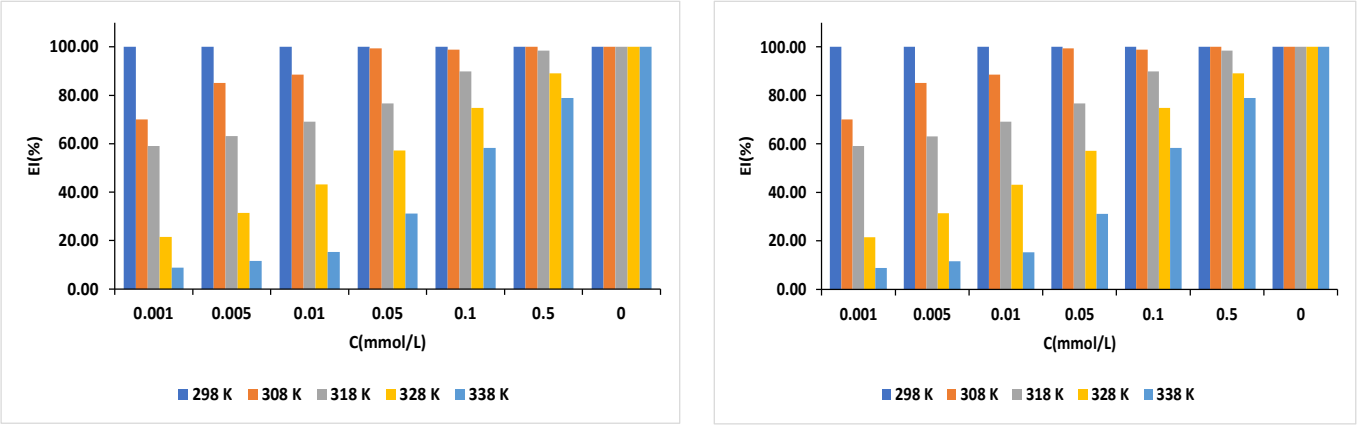

Figure 5. Band plot of the effectiveness of the 4Cl-BNH-NIP inhibitor as a function of concentration at a given temperature in an HCl medium.

These diagrams show that in a sulfuric acid medium, at a given temperature, the inhibition efficiency increases as the inhibitor concentration increases. In a similar study, the same result was obtained (20). According to the literature, an increase in the concentration of the inhibitory molecule means an increase in the number of molecules adsorbing onto the metal surface, thereby

reducing the metal area exposed to corrosion. Thus, in a sulfuric acid environment, 4ClBNH-NIP molecules better cover the metal surface to isolate it from the aggressive environment. Increasing the concentration increases the surface area of the protective film covering the metal surface (20).

Theoretical Study

Optimized Structures of the Molecule Using GaussView 6.0.16 : Using the GaussView 6.0.16 software, we obtained the optimized structure of our inhibitor molecule shown below:

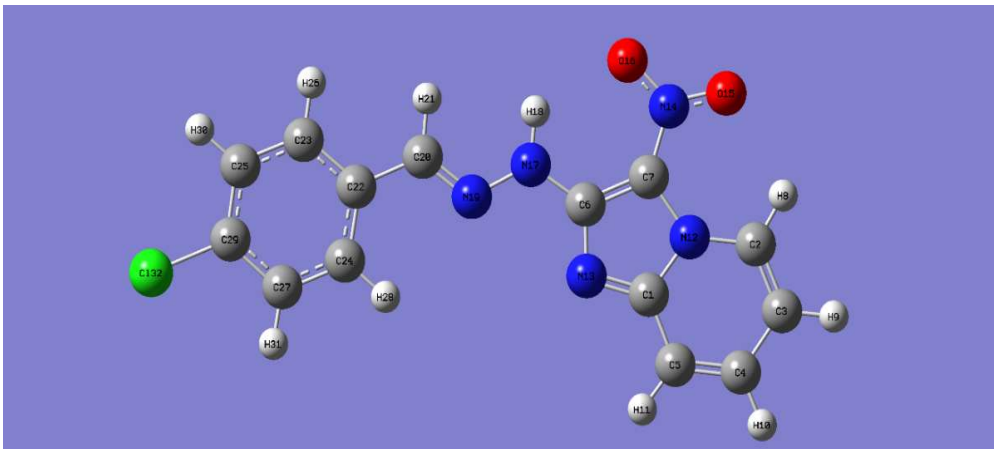

Figure 6. Optimized structure of 2-(2-(4-chlorobenzylidene)hydrazinyl)-3-nitroimidazo(1,2-α)pyridine.

HOMO and LUMO energy lobes of the molecules : The HOMO and LUMO energy lobes obtained using GaussView 6.0.16 for the molecule are shown below.

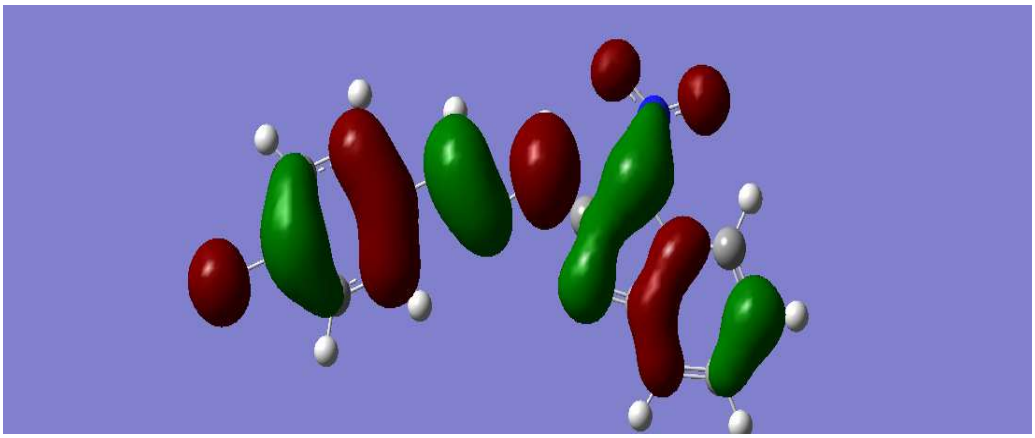

Figure 7. HOMO energy lobes of 2-(2-(4-chlorobenzylidene)hydrazinyl)-3-nitroimidazo(1,2-α)pyridine.

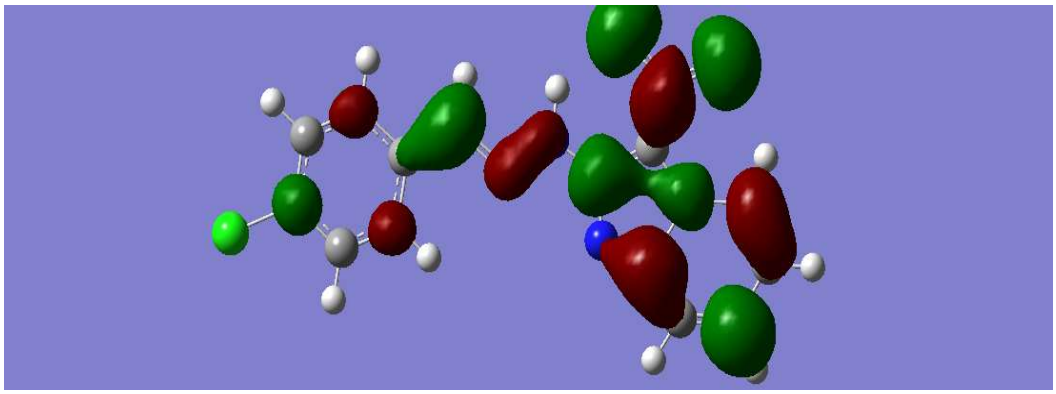

Figure 8. LUMO energy lobes of 2-(2-(4-chlorobenzylidene)hydrazinyl)-3-nitroimidazo(1,2-α)pyridine.

Descriptor parameters: The molecular descriptor parameters were calculated using Gaussian 09 with the B3LYP/6-311G (d,p) method. The calculated descriptors are listed in Table 1.

Table 1. Molecular descriptor parameters obtained from B3LYP/6-311G (d,p)

Descriptor	(E)-4ClBNH-NIP
E_{HOMO} (eV)	- 6.033856
E_{LUMO} (eV)	- 2.538824
Energy gap (ΔE) (eV)	3.495
Dipole moment μ (D)	3.371
Ionization energy I (eV)	6.034
Electron affinity A (eV)	2.539
Electronegativity χ (eV)	4.286339
Overall hardness η (eV)	1.748
Overall softness σ (eV^{-1})	0.572
Electron transfer fraction ΔN	-0.0018139
Electrophilicity index ω (eV)	5.257
Electron-accepting power ω+ (eV)	3.332
Electron-donating power ω- (eV)	7.618
Total energy ET (eV)	- 38750.5792

The 4ClBNH-NIP molecule exhibits a relatively high HOMO energy, indicating a moderate ability to donate electrons, in agreement with previously reported literature. It also shows a low LUMO energy, which reflects a strong ability to accept electrons. Furthermore, the molecule presents a small energy gap, characteristic of an efficient organic corrosion inhibitor. This small energy difference between the HOMO and LUMO orbitals therefore confirms its high chemical reactivity as well as its superior experimentally observed inhibition performance, particularly over a wide temperature range (21). The molecule also has a non-zero dipole moment, indicating a non-uniform distribution of electronic charges. This property promotes interactions with the metal surface (22). The hardness and softness parameters also show that this molecule is highly reactive with respect to the aluminum surface. Indeed, it has low hardness and high softness, which translates to a strong ability to interact with the metal (23). Furthermore, the electronegativity of 4ClBNH-NIP is higher than that of aluminum (4.28 eV). According to the literature, this difference indicates that the molecule attracts electrons from the aluminum metal (24). This observation is confirmed by the negative value of the electron transfer fraction ($\Delta N < 0$), indicating an electron transfer from aluminum to the molecule (25). Thus, (E)-4ClBNH-NIP behaves as a Lewis acid by accepting electrons from the metal surface to form a dative bond with aluminum (26). When the transfer fraction is less than 3.6, the inhibitory efficacy increases with the molecule's ability to accept or donate electrons, further confirming the excellent inhibitory performance of 4ClBNH-NIP.

Local reactivity parameters of the molecule: Table 2: Local descriptor parameters for the (E)-4ClBNH-NIP molecule in the B3LYP/6-311G(d,p) database

Molécule (E)-4ClBNH-NIP						
Atom	$qk(N+1)$	$qk(N)$	$qk(N-1)$	$fk(+)$	$fk(-)$	$\Delta fk(r)$
1 C	0.435765	0.419688	0.385631	0.016077	0.034057	-0.017980
2 C	0.180367	0.166661	0.144776	0.013706	0.021885	-0.008179
3 C	-0.217865	-0.247420	-0.265870	0.029555	0.018450	0.011105
4 C	0.053495	0.032509	-0.010088	0.020986	0.042597	-0.021611
5 C	-0.167140	-0.190167	-0.203741	0.023027	0.013574	0.009453
6 C	0.355888	0.350511	0.291120	0.005377	0.059391	-0.054014
7 C	0.388644	0.333052	0.321443	0.055592	0.011609	0.043983
8 H	0.189543	0.166117	0.141171	0.023426	0.024946	-0.001520
9 H	0.158823	0.121864	0.079619	0.036959	0.042245	-0.005286
10 H	0.150570	0.115698	0.070048	0.034872	0.045650	-0.010778
11 H	0.152379	0.124110	0.087025	0.028269	0.037085	-0.008816
12 N	-0.450531	-0.448930	-0.446549	-0.001601	-0.002381	0.000780
13 N	-0.318559	-0.345774	-0.360709	0.027215	0.014935	0.012280
14 N	0.165495	0.160633	0.118652	0.004862	0.041981	-0.037119
15 O	-0.257861	-0.321770	-0.432278	0.063909	0.110508	-0.046599
16 O	-0.315311	-0.351506	-0.454256	0.036195	0.102750	-0.066555
17 N	-0.276896	-0.349344	-0.339970	0.072448	-0.009374	0.081822
18 H	0.275420	0.248149	0.234450	0.027271	0.013699	0.013572
19 N	-0.135933	-0.160048	-0.182387	0.024115	0.022339	0.001776
20 C	0.212826	0.152020	0.089994	0.060806	0.062026	-0.001220
21 H	0.121525	0.074441	0.036414	0.047084	0.038027	0.009057
22 C	-0.174418	-0.160395	-0.143964	-0.014023	-0.016431	0.002408
23 C	-0.034869	-0.065928	-0.084187	0.031059	0.018259	0.012800
24 C	0.005204	-0.025822	-0.055474	0.031026	0.029652	0.001374
25 C	0.042519	0.021326	0.005800	0.021193	0.015526	0.005667
26 H	0.131016	0.096713	0.069573	0.034303	0.027140	0.007163
27 C	0.039952	0.020989	0.010036	0.018963	0.010953	0.008010
28 H	0.142250	0.118216	0.102264	0.024034	0.015952	0.008082
29 C	-0.219460	-0.232624	-0.250140	0.013164	0.017516	-0.004352
30 H	0.157719	0.120173	0.088070	0.037546	0.032103	0.005443
31 H	0.157274	0.122807	0.093995	0.034467	0.028812	0.005655
32 Cl	0.052168	-0.065949	-0.140467	0.118117	0.074518	0.043599

From this table, we observe that in the 4ClBNH-NIP molecule, oxygen (15 O) has the highest Fukui function f_k^- with a negative associated dual descriptor ($\Delta f_k < 0$), and that chlorine (32 Cl) has the highest function with a positive corresponding dual descriptor ($\Delta f_k > 0$). This molecule therefore has two attack sites: oxygen (15 O) and chlorine (32 Cl). Oxygen (15 O) is the nucleophilic site, while chlorine (32 Cl) is the electrophilic site in this molecule. Thus, an electrophilic attack is directed at oxygen (15 O), while a nucleophilic attack is directed at chlorine (32 Cl). In summary, during the adsorption process, the 4ClBNH-NIP molecule donates electrons to the metal around the oxygen (15 O) and accepts electrons from the metal around the chlorine (32 Cl) (27-28).

CONCLUSION

We can conclude that for our molecule, the corrosion inhibition efficiency increases with increasing concentration but decreases with rising temperature of the corrosive medium. The inhibitory efficacy is significant in a sulfuric acid environment Based on the local parameters determined using Gaussian 09W, we observe that 4ClBNH-NIP has two attack sites each: a nucleophilic site and an electrophilic site. Based on the global parameters, we also note that the molecule possesses excellent corrosion inhibition capacity and acts predominantly as an electron donor to the metal.

REFERENCES

Davis, J. R. (Ed.). (1999). *Corrosion of aluminum and aluminum alloys* (ASM International Handbook Series, Vol. 13A, 592 p.). Materials Park, OH: ASM International.

Polmear, I. J. (2006). *Light alloys: From traditional alloys to nanocrystals* (4th ed., 421 p.). Oxford, UK: Butterworth-Heinemann.

Fontana, M. G. (2005). *Corrosion engineering* (3rd ed., 880 p.). New York, NY: McGraw-Hill.

Revie, R. W., & Uhlig, H. H. (2008). *Corrosion and corrosion control: An introduction to corrosion science and engineering* (4th ed., 512 p.). Hoboken, NJ: John Wiley & Sons.

Landolt, D. (2007). *Corrosion and surface chemistry of metals* (615 p.). Lausanne, Switzerland: EPFL Press.

NACE International. (2016). *International measures of prevention, application, and economics of corrosion technologies study* (IMPACT, Report No. 7358, 144 p.). Houston, TX: NACE International.

Timoudan, N., et al. (2024). Corrosion inhibition performance of benzimidazole derivatives for protection of carbon steel in hydrochloric acid solution. *RSC Advances*, 14(41), 30295–30316.

Bentiss, F., Traisnel, M., & Lagrenée, M. (2000). The substituted 1,3,4-oxadiazoles: A new class of corrosion inhibitors of mild steel in acidic media. *Corrosion Science*, 42(1), 127–146.

ASTM International. (2004). *ASTM G31-72(2004): Standard practice for laboratory immersion corrosion testing of metals*. West Conshohocken, PA: ASTM International.

Ghamali, M., Chtita, S., Bouachrine, M., & Lakhlifi, T. (2016). Méthodologie générale d'une étude RQSA/RQSP. *Revue Interdisciplinaire*, 1(1), 1–6.

Adingra, K. F., Coulibaly, S., Alain, K., Ouattara, M., & Sissouma, D. (2022). Synthesis and anticandidosic activities of imidazo(1,2-a)pyridinyl derivatives. *Advances in Biological Chemistry*, 12(4), 81–91.

Khadom, A. A., Yaro, A. S., & Kadhum, A. A. H. (2010). Corrosion inhibition by naphthylamine and phenylenediamine for copper-nickel alloy in HCl. *Journal of the Taiwan Institute of Chemical Engineers*, 41(1), 122–125.

Musa, A. Y., et al. (2010). Kinetic behavior of mild steel corrosion inhibition by triazole derivative. *Journal of the Taiwan Institute of Chemical Engineers*, 41(1), 126–128.

Rahim, A. A., & Kassim, J. (2008). Vegetal tannins in corrosion protection of iron and steel. *Recent Patents on Materials Science*, 1(3), 223–231.

Geerlings, P., De Proft, F., & Langenaeker, W. (2003). Conceptual density functional theory. *Chemical Reviews*, 103(5), 1793–1874.

Dennington, R., Keith, T., & Millam, J. (2009). *GaussView Version 5*. Semichem Inc.

Frisch, M. J., et al. (2009). *Gaussian 09, Revision A.02*. Gaussian Inc.

Koffi, A. A., et al. (2023). Expired Fuclo 500 drug as corrosion inhibitor. *European Journal of Chemistry*, 14(3), 353–361.

Ehouman, A. D., et al. (2024). Aluminum corrosion in biogas environment. *Applied Chemical Engineering*, 7(3), ACE-5524.

Ahmed, A. A., et al. (2019). Triazole-based compound synthesis and gravimetric studies. *International Journal of Low-Carbon Technologies*, 15, 164–170.

Niamien, P. M., et al. (2010). Adsorption of benzimidazole derivatives in nitric acid. *Journal de la Société Ouest-Africaine de Chimie*, 30, 49–58.

Ehouman, A. D., et al. (2023). Thermodynamic study of piroxicam corrosion inhibition. *Earthline Journal of Chemical Sciences*, 10(2), 267–283.

Ahissan, D. E., et al. (2021). DFT study of tetrazole pyrimidine hybrids. *Oriental Journal of Chemistry*, 37(4), 805–812.

Mougo, A. T., et al. (2022). Benzimidazole derivative corrosion inhibition. *Mediterranean Journal of Chemistry*, 12(2), 123–139.

Mougo, A. T., et al. (2020). Sulfonylurea corrosion inhibition study. *Open Journal of Physical Chemistry*, 10, 139–157.

Kouakou, V., et al. (2021). Methylxanthines corrosion inhibition study. *Journal of Pure and Applied Chemistry Research*, 10(1), 1–17.

Lewars, E. G. (2011). *Computational chemistry: Introduction to the theory and applications of molecular and quantum mechanics* (2nd ed.). Springer.

Fuentealba, P., Perez, P., & Contreras, R. (2000). On the condensed Fukui function. *The Journal of Chemical Physics*, 113(7), 2544–2551.

Beda, R. H. B., et al. (2017). Caffeine as corrosion inhibitor of aluminum in HCl. *Advances in Chemistry*, 2017, 1–10

****